Solid State Communications 149 (2009) 1905–1908

Contents lists available at ScienceDirect

Solid State Communications

journal homepage: www.elsevier.com/locate/ssc

Swift heavy ion irradiation induced phase transformation in calcite single crystals

H. Nagabhushana [a,*,1], B.M. Nagabhushana [b], B.N. Lakshminarasappa [c], Fouran Singh [d], R.P.S. Chakradhar [e]

[a] Department of PG Studies in Physics, Govt. Science College, Tumkur-572 103, India
[b] Department of Chemistry, M.S. Ramaiah Institute of Technology, Bangalore-560 054, India
[c] Department of Physics, Bangalore University, Bangalore-560 056, India
[d] Inter University Accelerator Centre, Aruna Asaf Alimarg, New Delhi - 110 067, India
[e] Glass Technology Lab, Central Glass and Ceramic Research Institute (CSIR), Kolkata- 700 032, India

ARTICLE INFO

Article history:
Received 27 May 2009
Received in revised form
16 July 2009
Accepted 30 July 2009 by P. Sheng
Available online 3 August 2009

PACS:
87.64je
80.00jh

Keywords:
A. Quasicrystals
C. Dislocations and disclinations
D. Phase transitions
E. Atom, molecule, and ion impact

ABSTRACT

Ion irradiation induced phase transformation in calcite single crystals have been studied by means of Raman and infrared spectroscopy using 120 MeV Au^{9+} ions. The observed bands have been assigned according to group theory analysis. For higher fluence of 5×10^{12} ion/cm^2, an extra peak on either side of the 713 cm^{-1} peak and an increase in the intensity of 1085 cm^{-1} peak were observed in Raman studies. FTIR spectra exhibit extra absorption bands at 674, 1589 cm^{-1} and enhancement in bands at 2340 and 2374 cm^{-1} was observed. This might be due to the phase transformation from calcite to vaterite. The damage cross section (σ) for all the Raman and FTIR active modes was determined. The increase of FWHM, shift in peak positions and appearance of new peaks indicated that calcite phase is converted into vaterite.

1. Introduction

When swift heavy ions (SHI) pass through a solid target, a considerable amount of energy is transferred by the collisions with the electrons of the target material, resulting in transient high energy densities along the ion paths. The knocked out electrons, in turn, either dissipate their energy by collisions with other electrons or by electron–phonon coupling. High energy densities are known to be a prerequisite for phase transitions, which have occasionally been found to occur along swift heavy ion tracks [1,2]. Calcium carbonate occurs in three main crystalline polymorphs (calcite, aragonite, and vaterite), in two hydrated crystal forms (calcium carbonate monohydrate and calcium carbonate hexahydrate), and also as an amorphous material [3]. Calcite is the most abundant form and is widely distributed in the earth's crust followed by aragonite and vaterite. From the thermodynamic viewpoint, calcite is more stable than the other two structures at room temperature and atmospheric pressure, whereas vaterite is the most unstable polymorph which is rarely seen. Calcium carbonate has been widely used as a model system for investigating inorganic precipitation reaction or crystallization due to its important industrial application in paints, plastics, rubber, paper, cosmetics, and food industries [4].

Calcite has a trigonal structure with two molecules per unit cell. The calcium ions and the carbon atoms of the carbonate ions all lie on the trigonal axis and the orientations of the two carbonate ions are staggered relative to each other so that there is a center of symmetry. The structure of calcite is of greater interest because of a number of important mineral constituents of sedimentary rocks, including magnesium and iron bearing carbonate, having structures that are identical with or closely related to the calcium pattern [5]. Therefore, the structure of calcite serves as a logical starting point in describing the structure of such materials.

Some studies have been carried out on phase transformation of calcite to other phases including ball milling [6], temperature, pressure [7,8], hydrothermal synthesis [9] etc. Previous works [7,8] from IR and Raman studies on calcite crystals have demonstrated that carbonate internal modes were sensitive to the phase changes from temperature and pressure and could effectively be used to probe the structural transitions. However, to the best of our

* Corresponding author. Tel.: +91 080 23146895; fax: +91 0816 2260220.
E-mail addresses: bhushanvl@rediffmail.com (H. Nagabhushana), sreechakra72@yahoo.com (R.P.S. Chakradhar).
[1] Mobile No: 9945954010.

0038-1098/$ – see front matter © 2009 Elsevier Ltd. All rights reserved.
doi:10.1016/j.ssc.2009.07.049

knowledge phase transformation of calcite using swift heavy ion irradiation has not been reported. In the present work, an attempt has been made to study 120 MeV Au^{9+} ion irradiation induced effects on CO_3^{2-} internal modes in the $CaCO_3$ single crystals by means of Raman and FTIR spectroscopy.

2. Experimental

Transparent calcite single crystals of $\sim 1\times1\times2$ mm^3 are cleaved in a big block procured from Alminrock minerals, Bangalore, India. The samples are irradiated at room temperature over an area 1×1 cm^2 by scanning the ion beam using an electromagnetic scanner. The vacuum in the irradiation chamber is maintained at $\approx 10^{-6}$ Torr. Au^{9+} ions of 120 MeV are used to irradiate the calcite single crystals from 15-UD Pelletron at Inter University Accelerator Centre, New Delhi [10] with appropriate beam current of 2Pna. The fluences used are 1×10^{11}–5×10^{12} ions/cm^2. Raman spectroscopic studies are carried out on the pristine (without irradiation) and Ag^{9+} ion irradiated crystals using a *Renishaw* In via Raman spectrometer with 785 nm He–Cd laser operating at 150 W power. Leica DMLM optical microscope equipped with 50X objective lens is used to determine the analyzed part of the sample. Three to five accumulations for each position with an accumulation time of 10 s are maintained for all the measurements. The spectra are calibrated using 520 cm^{-1} line of silicon wafer. The data acquisition and analysis are carried out using *WIRE 2.0* software. The FTIR measurements of pristine and ion irradiated calcite single crystals are carried out using Bruker FTIR instrument from 400–3500 cm^{-1}.

3. Results and discussion

Raman spectroscopy is known to be a nondestructive material characterization technique. It provides a unique way of probing surface and structural properties of ion beam modified materials. According to factor group analysis 27 optical modes will be distributed (lattice modes, internal modes) [11]. In Raman spectrum of calcite, a total of five fundamental vibrational modes, two lattice modes and three internal modes are expected to be active [12] along with overtone of the infrared active $2\upsilon_2$ mode at 1759 cm^{-1}. Fig. 1 shows the Raman spectra of pristine and 120 MeV Au^{9+} ion irradiated calcite single crystals for a fluence of 1×10^{11}–5×10^{12} ions/cm^2. The pristine spectrum has five fundamental bands located at $\sim$152, 280, 713, 1085 and 1485 cm^{-1} along with extra bands located at 1118, 1203, 1291, 1382, 1542, 1659, 1759 and 1841 cm^{-1}. These fundamental bands are in good agreement with those reported in the literature [13–16]. From factor group analysis of calcite, internal A_{1g} mode (υ_1, symmetric stretch) of the carbonate anion located at $\sim$1085 cm^{-1} is the strongest feature. The weak lines located in the regions of 1485 and 713 cm^{-1} are due to internal E_g modes corresponding to the in-plane bending (υ_4) and anti-symmetric stretching (υ_3) modes of CO_3^{2-} ions. The two small bands at 152 and 280 cm^{-1} have been assigned to translational and rotational (E_g) modes respectively. The overtone band at $\sim$1759 cm^{-1} is an A_{1g} internal mode corresponding to out-of-plane bending (υ_2). The strong Raman vibrational band at 1085 cm^{-1} corresponding to the case in which all the CO_3^{2-} groups vibrate as in identical phases [17]. The band at 1542 cm^{-1} (υ_1) which is produced by the stretching vibration of –C=C– double bonds, and at 1118 cm^{-1} (υ_1) stretching of –C–C– single bonds [18].

Liu et al. [19] have studied the phase transformation of calcite by Raman spectra in hydrostatic pressure environment. They observed most intense band at $\sim$1085 cm^{-1} (A_{1g} mode), two sets of doubly degenerate, internal E_g modes (712 and 1434 cm^{-1}) and

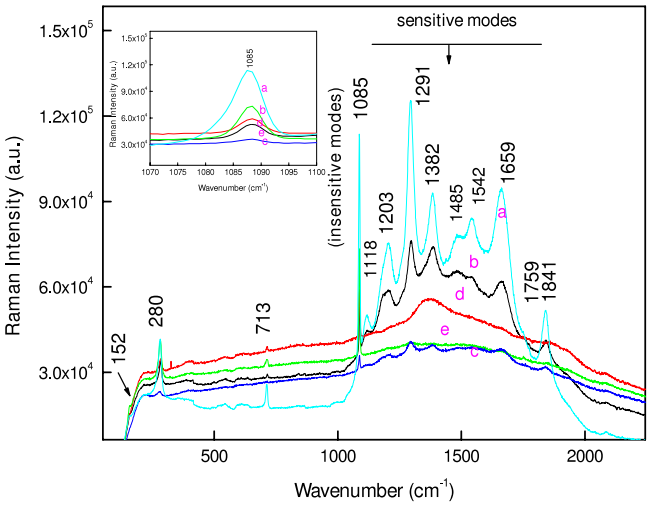

Fig. 1. Raman spectra of (a) Pristine (b) 1×10^{11} ions cm^{-2} (c) 5×10^{11} ions cm^{-2} (d) 1×10^{12} ions cm^{-2} (e) 5×10^{12} ions cm^{-2} (inset: The 1085 cm^{-1} peak increase as the Au^{9+} ion fluence 5×10^{12} ions cm^{-2} (dotted line)).

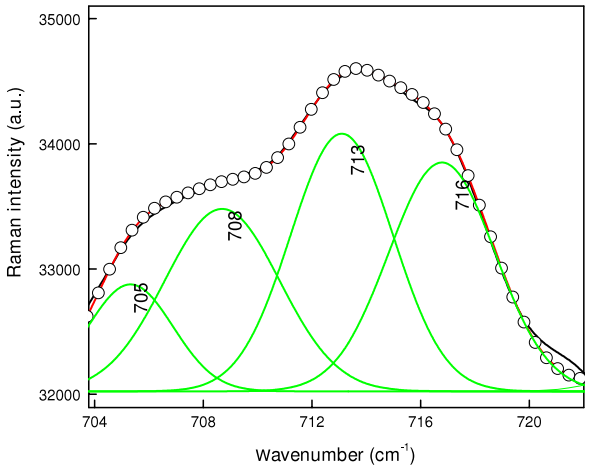

Fig. 2. Deconvolution of 713 cm^{-1} peak (5×10^{12} ions cm^{-2}).

external E_g or lattice modes (282 and 156 cm^{-1}). The external modes are associated with liberation of the CO_3^{2-} ions in primitive cell around axes normal to the C_3 axis and translations of the CO_3^{2-} ions normal to the C_3 axis, respectively. At high pressures, the bands at 1440 and 715 cm^{-1} splits into doublets. This is an indication of phase transformation. Krishnamurthi et al. [20] have studied the calcite crystal by Raman spectroscopy. The strong Raman band at 1092 cm^{-1} corresponding to the case in which all the CO_3^{2-} group vibrate in identical phase. The strong Raman active modes 1092 cm^{-1} would combine with weak modes 162, 288, 716 and 1437 cm^{-1} to give sharply defined symmetrical values.

In the present study, it is observed that the intensity of the sensitive Raman modes decreases with increase of ion fluence (1×10^{11}–5×10^{12} ions/cm^2). With increase of ion fluence to 5×10^{12} ions/cm^2, the sensitive Raman bands completely disappear and the modes at 1085 (inset of Fig. 1) and 713 cm^{-1} start growing with additional features arising at 713 cm^{-1} peak. In order to identify the extra bands produced after irradiation, we deconvoluted the peak using *ORIGIN 8.0* software. The results indicate that the asymmetric peak is nicely presented as a mixture of three Gaussian peaks at 705, 708 and 716 cm^{-1} respectively (two from lower wave number side and one from higher wave number side) (Fig. 2).

Increase of FWHM and area under the peak, peak shift towards higher wave number side as well as presence of new peaks at

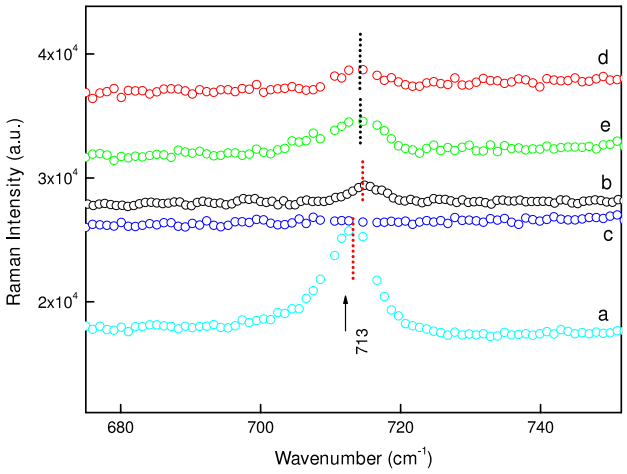

Fig. 3. Peak shift (713 cm^{-1}) with the increase of Au^{9+} ion irradiation (a) Pristine (b) 1×10^{11} ions cm^{-2} (c) 5×10^{11} ions cm^{-2} (d) 1×10^{12} ions cm^{-2} (e) 5×10^{12} ions cm^{-2}.

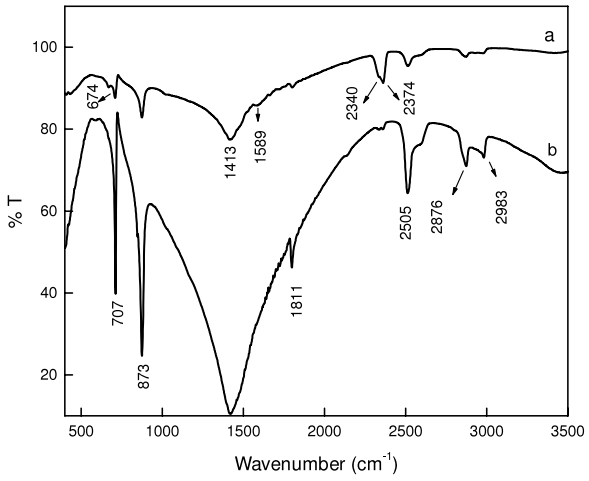

Fig. 4. FTIR spectra of (a) Au^{9+} ion irradiated (5×10^{12} ions cm^{-2}) (b) Pristine.

713 cm^{-1} were observed (Fig. 3) with increase of ion fluence. This is a strong evidence of phase transformation of calcite. The decrease in intensity of sensitive Raman bands with increase of ion fluence might be due to breakage of CO_3^{2-} ions due to amorphization/ either change in the crystal phase or surface amorphization. Amorphization occurs because each incident ion creates one or several different cascades which become amorphous as a result of the rapid quenching and these cascades eventually overlap to form an amorphous solid [19].

Benyagoub et al. [21] have studied phase transformation induced in pure zirconia by high energy heavy ions with ^{58}Ni (550, 300, 135 MeV) and ^{76}Ge (300 MeV). The phase transformation was studied by means of XRD and Raman spectroscopy. The experiments clearly confirm that the irradiation of pure zirconia with swift heavy ions can induce a crystalline phase transformation from monoclinic to tetragonal phase. It is demonstrated that this transformation is triggered only when the deposited electronic energy loss is in excess of a threshold ~13 keV nm^{-1}. If electronic energy loss is less than the threshold, amorphization, defect and track formation were observed. From transport of ions in matter (TRIM) calculations, when the energy of the incident ions is of few keV then the nuclear energy loss (S_n) are significant as compared to electronic energy loss (S_e). In the present experiment we have used 120 MeV energy for irradiation and the nuclear energy is dominant over the electronic energy transfer interactions in the near surface region. Therefore, there is a possibility of phase transformation of calcite.

FTIR studies have been carried out to confirm the phase transformation/surface amorphization. Fig. 4 shows the FTIR spectra of pristine and Au^{9+} ion irradiated calcite for a fluence of 5×10^{12} ions/cm^2. The main absorption peaks observed at ~707, 873, 1413, 2505, 2876, 2983 cm^{-1}. In the FTIR spectra, out-of-plane bending (υ_2), the asymmetric stretching (υ_3) and in-plane bending (υ_4) modes of CO_3^{2-} ions and found to be active as predicted from the factor group analysis [17]. Besides the first order internal modes the $\upsilon_1 + \upsilon_4$, $2\upsilon_2 + \upsilon_4$, $2\upsilon_3$ combinational modes are observed. The presence of non-splitting peaks υ_2 and υ_4 in the pristine sample indicate the presence of calcite structure in the sample.

It is observed from the figure, in ion irradiated sample, an extra absorption bands at 674 and 1589 cm^{-1}, at the same time the other absorption bands completely destructed with increase of ion fluence. The destruction of these modes with irradiation may further enhance the amorphous in nature of the sample. The decrease in (Raman and FTIR) intensity might

Table 1
Observed frequencies in Raman and FTIR spectra of calcite.

Raman	FTIR	Assignment
152 (m)	–	LM calcite
280 (m)	–	LM calcite
713 (w)	707 (w)	υ_4-CO_3 calcite
1085 (s)	873 (m)	υ_2-CO_3 calcite
1485 (w)	1413 (s, b)	υ_3-CO_3 calcite
1759 (w)	1811 (sh)	$\upsilon_1 + \upsilon_4$
–	2505 (m)	$2\upsilon_2 + \upsilon_4$
–	2776–2983 (m)	$2\upsilon_3$

m: medium, w: weak, s: strong, b: broad, sh: shoulder, LM: Lattice mode, υ_1-symmetric stretching, υ_2-symmetric bending, υ_3-asymmetric stretching, υ_4-asymmetric bending.

be attributed to the destruction of the surface chemical species (CO_3^{2-}) because of the energy deposited through S_e during SHI irradiation and formation of non-radiative recombination centers at higher fluences. The irradiation effects may lead to the restructuring of the chemical species because of the energy deposited through electronic energy loss during the process of SHI irradiation and formation of ion induced defects leading to non-radiative recombination centers. These two processes are simultaneous consequences of irradiation and they compete with each other [22]. The degradation/enhancement in Raman peaks intensity might be due balance between these two effects. The mode assignments of fundamental bands in FTIR and Raman studies are given in Table 1.

Shivakumar et al. [23] have studied the synthesis of vaterite phase by direct precipitation of glycine and L-alanine. They observed a characteristic CO_3^{2-} peak at 1417 cm^{-1} and C–O stretching at 1084 and 713 cm^{-1} in FTIR measurements. In pure vaterite characteristic CO_3^{2-} at 1417 cm^{-1} splits into 1478 and 1406 cm^{-1}. The C–O stretching appear at 744 cm^{-1} in pure vaterite and common C–O stretching at around 1084 and 713 cm^{-1} due to mixed phase. In vaterite phase the peaks at 1084 and 671 cm^{-1} are more prominent when compared to calcite.

The damage cross section (σ) for the destruction of the $CaCO_3$ can be observed from the decrease in the Raman peak intensity as a function of Au^{9+} ion dose. Following the analysis suggested in [24] we assume that the areal density N of the $CaCO_3$ molecule remaining after irradiation with an ion dose D is given by

$$N = N_0 \exp(-\sigma D)$$

where σ is the cross section. For the Raman measurements, N is proportional to the integrated Raman intensity Hence, for the Raman measurements a plot of $\log_{10}[I(D)/Io]$ versus dose where

I(D) is the intensity of a particular Raman peak after a dose D and Io is the intensity of the corresponding peak in the pristine sample, should yield a straight line whose slope is the cross section, σ for the destruction of $CaCO_3$ by the ion beam. The intensity of the different Raman bands after a given dose I(D), normalized to the intensity of this peak for pristine sample Io is plotted as $\log_{10}$[I(D)/Io] versus ion fluence. The Raman data when plotted in this way do indeed follow a straight-line dependence. The linear fits to Raman data yield a damage cross section (σ) of different Raman modes. The errors have been estimated on the basis of lines of worst fit taking into account the uncertainties in each of the data points. It is noticed that all the fundamental Raman active modes having different damage cross sections/different sensitiveness for ion irradiation. The sensitive Raman modes such as 1118, 1203, 1291, 1382, 1485, 1542, 1659, 1759 and 1841 cm^{-1} have highest damage cross section ($\sim 2.2 \times 10^{12}$ cm^2) i.e. the most sensitive to get damaged by ion beam. On the other hand the 1085, 280 cm^{-1} modes have lowest damage cross section (1.0×10^{-12} cm^{-2}). This is the least affected vibrational mode. Atomic Force microscopy (AFM) and glancing angle X-ray diffraction (G-XRD) are effective tools for examining surface modifications/ phase transformation of the sample.

4. Conclusions

The Raman and Infrared spectroscopic studies of 120 MeV Au^{9+} swift heavy ion irradiated calcite single crystals have been studied in the fluence range 1×10^{11}–5×10^{12} ions/cm^2. The characteristic Raman bands observed at ~152, 280, 713, 1085 and 1485 cm^{-1} respectively. In FTIR spectrum, the main absorption bands observed at ~707, 873, 1413 and 1811 cm^{-1} respectively. It is observed that intensity, area, FWHM of the Raman and FTIR sensitive peaks decreases with increase in Au^{9+} ion fluence. For higher fluence of 5×10^{12} ion/cm^2, an extra peak on either side of the 713 cm^{-1} peak and increase in intensity of 1085 cm^{-1} peak was observed in Raman studies. Whereas in FTIR studies, extra absorption bands at 674, 1589 cm^{-1} and enhancement in absorption bands at 2340 and 2374 cm^{-1} was observed. This might be due to the phase transformation from calcite to vaterite. The damage cross section (σ) for all the Raman and FTIR active modes were determined and found to be different for different modes. The increase of FWHM, shift in peak positions and appearance of new peaks indicated that calcite phase is converted into vaterite.

Acknowledgments

The authors wish to express their sincere thanks to Dr. D.K. Avasthi, Nuclear Science Centre (NSC), New Delhi, for useful discussion, besides his constant help and encouragement in this work. One of the authors (H.N.) thanks to NSC for the award of Fellowship under UFUP scheme. Dr. RPSC thanks Dr. H.S. Maiti, Director CGCRI and Dr. R. Sen, Head GTL lab for their constant support and encouragement.

References

[1] Lakhwant Singh, K.S. Samra, Ravinder Singh, Indra Solania, D.K. Avasthi, J. Non. Cryst. Solids 354 (2008) 41.
[2] H. Nagabhushana, B. Umesh, B.M. Nagabhushana, B.N. Lakshminarasappa, Fouran Singh, R.P.S. Chakradhar, Spectrochim. Acta A 73 (2009) 637.
[3] Hua Tang, Jiaguo Yu, Xiufeng Zhao, Mater. Res. Bull. 44 (2009) 831.
[4] E. Dalas, P. Klepetsanis, P.G. Koutsoukos, Langmuir 15 (1999) 8322.
[5] Danhua Lou, Fengjiu Sun, Lijuan Li, Chin. Opt. Lett. 5 (2009) 370.
[6] A. Devarajan, M. Abdul Khadar, K. Chattopadhyay, Mat. Sci. Eng. A 452 (2007) 395.
[7] Philippe Gillet, Claudine Biellmann, Bruno Reynard, Paul McMillan, Phys. Chem. Mineral. 20 (1993) 1.
[8] M.Y. Fong, M. Nicol, J. Chem. Phys. 54 (1971) 579.
[9] Z. Nan, X. Chen, Q. Yang, X. Wang, Z. Shi, W. Hou, J. Colloid Interface Sci. 325 (2008) 331.
[10] G.K. Mehta, A.P. Patro, Nucl. Instrum. Methods A 268 (1998) 334.
[11] J. Urmos, S.K. Sharma, F.T. Mackenzie, Am. Mineral. 76 (1991) 641.
[12] W.B. White, The Carbonate Minerals, Mineralogical Society, London, 1974.
[13] Akio Yammoto, Yuji Shiro, Hiromu Murata, Bull. Chem. Soc. Jpn. 47 (1974) 265.
[14] C.G. Kontoyannis, N.V. Vagenas, Analyst 125 (2000) 251.
[15] H.N. Rutt, J.H. Nicola, J. Phys. C Solid State 7 (1974) 4522.
[16] S. Gunasekaran, G. Anbalagan, Spectrochim. Acta A 68 (2007) 656.
[17] S. Gunasekaran, G. Anbalagan, Spectrochim. Acta A 69 (2008) 1246.
[18] S. Saito, M. Tasumi, J. Raman Spectrosc. 14 (1983) 310.
[19] Lin-Gun Liu, T.P. Mernagh, Am. Minerol. 75 (1990) 801.
[20] D. Krishnamurthi, Proc. Indian Acad. Sci. A 46 (1957) 183.
[21] A. Benyagoub, F. Couvreur, S. Bouffard, F. Levesque, C. Dafour, E. Paumier, Nucl. Instrum. Methods B 175–177 (2001) 417.
[22] T.M. Bhave, S.S. Hullavarad, S.V. Bhoraskar, S.G. Hegde, D. Kanjilal, Nucl. Instrum. Methods B 156 (1999) 121.
[23] C. Shivakumara, Pretam Singh, Asha Gupta, M.S. Hegde, Mater. Res. Bull. 41 (2006) 1455.
[24] S. Prawer, K.W. Nugent, S. Biggs, D.G. McCulloch, W.H. Leong, A. Hoffman, R. Kalish, Phys. Rev. B 52 (1995) 841.